Research Article Vol. 43, No. 1 / January 2026 / Journal of the Optical Society of America B 159

Journal of the Optical Society of America B

OPTICAL PHYSICS

Optical nonlinearity of a cold atomic ensemble driven by a strong coherent field in a saturation regime

A. S. Usoltsev,[1,2] L. V. Gerasimov,[1,2] A. D. Manukhova,[3] S. P. Kulik,[1] and D. V. Kupriyanov[1,2,4,*]

[1]Quantum Technology Centre, M.V. Lomonosov Moscow State University, Leninskiye Gory 1-35, 119991 Moscow, Russian Federation
[2]Centre for Interdisciplinary Basic Research, HSE University, St. Petersburg 190008, Russian Federation
[3]Department of Optics, Palacký University, 17 Listopadu 12, 771 46 Olomouc, Czech Republic
[4]Department of Physics, Old Dominion University, 4600 Elkhorn Avenue, Norfolk, Virginia 23529, USA
*kupriyanov@quantum.msu.ru

Received 23 September 2025; revised 15 November 2025; accepted 15 November 2025; posted 24 November 2025; published 15 December 2025

We present a microscopic analysis and evaluation of the dielectric susceptibility of a dielectric medium consisting of vector-type two-energy-level atoms, responding to a weak probe mode, when the atoms are driven by a strong coherent field. Each atom, in an environment of others, exists as a quasiparticle, further structuring the bulk medium. In a limit of dilute atomic gas, the dynamics of each atom follows the Mollow-type nonlinear excitation regime, and the medium susceptibility collectivizes the individual atomic responses to the probe mode. We outline how the collective dynamics can be interpolated up to a dense medium, and we argue from general positions that in such a medium, the optical nonlinearity and, in particular, its parametric part could be significantly magnified by manipulating both the coherent pump and the sample density. This indicates certain limitations for potential capabilities of quantum communication protocols utilizing entangled photons created by a parametric process as a main resource of quantum correlations.

https://doi.org/10.1364/JOSAB.580004

1. INTRODUCTION

Optical nonlinear susceptibilities $\chi^{(n)}$, where $n \geq 2$, determine how a medium responds to an intense light field by generating new harmonics, mixing frequencies, or creating entangled photon pairs. In particular, in quantum communications, they are responsible for the generation of entangled photons in a spontaneous parametric down-conversion or four-wave mixing, for signal transformation in quantum repeaters, for frequency conversion, providing compatibility with telecom networks, and for implementation and rejection of a photon number splitting attack [1].

However, the practical implication of optical nonlinearities to quantum communications meets both fundamental and technical limitations: (a) Phase noise, accompanying the preparation of photons by a parametric process, reduces the fidelity of the transfer of quantum states. In an example of a quantum repeater, adjusted with a twin-field-quantum-key-distribution protocol, the phase noise from the $\chi^{(2)}$ light source, using $LiNbO_3$ crystals, limits the communication range by ∼500 km [2]; (b) at higher pump powers, uncontrolled multi-photon absorption adds a risk of optical damage to any communication protocol; and (c) in practical realizations, the achievable levels of nonlinearities are limited by available materials and by existing experimental capabilities [3–5].

In this regard, the question naturally arises: what are the physical limits of optical nonlinearities in the preparation of multi-photon states feasible for quantum communications? In general, for unspecified nonlinear optical materials, the answer would depend on many peculiar matter properties and be non-obvious. Nevertheless, to clarify the most critical requirements, one can attempt to find an appropriate theoretical model that allows for a microscopic description under realistic external conditions, and a cold atomic ensemble seems to be a relevant example of such a model.

The fundamental quantum properties of an atom-field interaction in the regime of nonlinear excitation by a strong coherent field were clarified in seminal papers [6,7] and are now commonly referred to as the Mollow problem. Decades later, the nonlinear coupling in the four-wave mixing in sodium vapor was utilized in the first experiment demonstrating the light squeezed by a parametric process developing under non-degenerate conditions in a cavity, in [8] and theoretically described in [9]. Recently, the concept of using four-wave mixing in cold alkali-metal atoms as a convenient technical

tool for the generation of narrow-band spectrally distributed entangled photons has been revived and actively studied in experiments [10,11]. Higher orders of optical nonlinearity have been observed in spontaneous parametric scattering in experiments with hot and dense atomic vapors in [12,13].

Independently, an application of the Mollow problem to light transport, driven by a coherent control field, in ultracold optically dense atomic systems has been investigated experimentally and theoretically in works [14–19]. The main attention of those papers was focused on interference phenomena, namely, weak and strong localizations of light in disordered atomic gas under conditions of incoherent emission. Specific examples of a light amplifier and a random laser without inversion, driven by a coherent pump on a closed transition in an optically dense atomic gas, were proposed in [20–22]. Despite these, to our knowledge, the complete vector description of Mollow nonlinearity in an atomic medium is still an open issue for theory.

Here we aim to construct a nonlinear dielectric susceptibility of a cold atomic ensemble by applying a consistent microscopic approach from the beginning to the end of our derivation sequence, i.e., in a maximally rigorous fashion. Our strategic motivation is to clarify, from fundamental microscopic positions framed by our model, an option for maximal enhancement of the system's nonlinear parametric response to a weak signal mode. For this, we consider an example of a four-wave mixing process developing in a dielectric medium consisting of cold atoms having a closed optical transition. For such a system: (i) the light and matter have the strongest coupling, and (ii) the closed transition works maximally effectively for the creation of nonlinearity with four-wave mixing ranging from weak to saturation regimes.

The paper is organized as follows. In Section 2 of this paper and Section 1 of Supplement 1, we present a microscopic derivation of the macroscopic Maxwell equations in the Heisenberg formalism, valid in the assumption of a long-wavelength dipole gauge. In Section 3, we simplify our consideration by a dilute system and derive the Kubo formula in the case of optical nonlinearity, which expresses the susceptibility tensor via Heisenberg dynamics of the atomic dipoles driven by a strong coherent field. For such conditions, in Section 4 of this paper and Section 2 of Supplement 1, we present the consistent derivation of the susceptibility tensor. Our calculations of the Kerr-type and parametric-type nonlinearities as functions of the saturation parameter are presented in Section 5. An extension of the reported results up to a dense system, structuring a bulk dielectric medium, is outlined in Section 6. Finally, we summarize our concluding remarks.

2. MACROSCOPIC MAXWELL EQUATIONS IN THE HEISENBERG FORMALISM

The physical concept, which we shall follow, implies the joint atom-field dynamics of the electromagnetic field existing in an arbitrary state and interacting with an atomic medium. The field can be both strong and weak, so that in certain modes it could saturate the atomic transitions. However, it does not dramatically distort the atomic energy structure and leaves the atom as a stable physical unit. The medium consists of atoms having ground and excited states belonging to a separated dipole-type optical transition.

Under these conditions, and for many applications, the interaction process can be approximated by a long-wavelength dipole-type interaction. Since the dipole-type interaction, or dipole gauge, is only approximately valid, its practical use can lead to some variations in the layout of the dynamical equations, which are featured by our derivation steps clarified in Section 1 of Supplement 1. That would be most important for dense samples, but even in a dilute regime, when the atoms are separated by distances scaled by their radiation zones, it would be wise to summarize them and clarify our starting position.

The Heisenberg precursor of the macroscopic Maxwell equations can be written in two equivalent forms. First, the Heisenberg equations can be written as coupled operator dynamics for the transverse components of the electric field $\hat{\mathbf{E}}_\perp(\mathbf{R}, t)$ and magnetic field $\hat{\mathbf{B}}(\mathbf{R}, t)$, which are considered as functions of spatial point $\mathbf{R}$ and time t:

$$\begin{aligned} \mathrm{rot}\,\hat{\mathbf{B}}(\mathbf{R}, t) &= \frac{1}{c}\dot{\hat{\mathbf{E}}}_\perp(\mathbf{R}, t) + \frac{4\pi}{c}\dot{\hat{\mathbf{P}}}_\perp(\mathbf{R}, t), \\ \mathrm{rot}\,\hat{\mathbf{E}}_\perp(\mathbf{R}, t) &= -\frac{1}{c}\dot{\hat{\mathbf{B}}}(\mathbf{R}, t), \end{aligned} \tag{2.1}$$

where

$$\hat{\mathbf{P}}_\perp(\mathbf{R}, t) = \sum_{a=1}^{N} \hat{\mathbf{d}}_\perp^{(a)}(\mathbf{R}, t) \tag{2.2}$$

is the transverse component of the microscopic collective dipole density, where the sum is taken over all N-atoms of the ensemble. The transversality means orthogonality to the wave vectors $\mathbf{k}$ of each field mode $s = \mathbf{k}, \sigma$ with polarization vectors $\mathbf{e}_s \equiv \mathbf{e}_\sigma(\mathbf{k})$ $(\sigma = 1, 2)$, such that in the Schrödinger picture for an ath dipole it is given by

$$\hat{\mathbf{d}}_\perp^{(a)}(\mathbf{R}) = \frac{1}{\mathcal{V}} \sum_s \mathbf{e}_s \cdot \left(\mathbf{e}_s \cdot \hat{\mathbf{d}}^{(a)}\right) \mathrm{e}^{i\mathbf{k}\cdot(\mathbf{R}-\mathbf{R}_a)}, \tag{2.3}$$

where $\mathbf{R}_a$ is the spatial location of the ath atomic dipole and $\mathcal{V}$ is a quantization volume.

Alternatively, Eq. (2.1) can be rewritten as

$$\begin{aligned} \mathrm{rot}\,\hat{\mathbf{B}}(\mathbf{R}, t) &= \frac{1}{c}\dot{\hat{\mathbf{D}}}(\mathbf{R}, t), \\ \mathrm{rot}\,\hat{\mathbf{E}}_{\mathrm{tot}}(\mathbf{R}, t) &= -\frac{1}{c}\dot{\hat{\mathbf{B}}}(\mathbf{R}, t), \end{aligned} \tag{2.4}$$

where we have introduced the components of the total electric and displacement fields. Their Schrödinger originals are, respectively, given by

$$\begin{aligned} \hat{\mathbf{E}}_{\mathrm{tot}}(\mathbf{R}) &= \hat{\mathbf{E}}_\perp(\mathbf{R}) + \sum_{a=1}^{N} \hat{\mathbf{E}}_{\mathrm{dip}}^{(a)}(\mathbf{R}), \\ \hat{\mathbf{D}}(\mathbf{R}) &= \hat{\mathbf{E}}_\perp(\mathbf{R}) + 4\pi\hat{\mathbf{P}}_\perp(\mathbf{R}), \\ &= \hat{\mathbf{E}}_{\mathrm{tot}}(\mathbf{R}) + 4\pi \sum_{a=1}^{N} \hat{\mathbf{d}}^{(a)}\delta(\mathbf{R}-\mathbf{R}_a), \end{aligned} \tag{2.5}$$

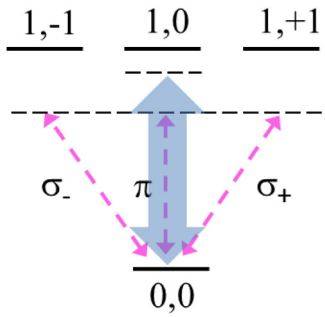

Fig. 1. Energy structure of a V-type tripod atom constructing the medium used in our simulation of the dielectric sample. The Zeeman states are specified by the angular momentum and its projection. The shaded arrow indicates the strong field quasi-resonant to the reference transition. The three dashed arrows belong to a weak probe impinging on the atom from an arbitrary direction and superposed in the atomic basis. The probe is detuned from both the atomic transition and coherent mode.

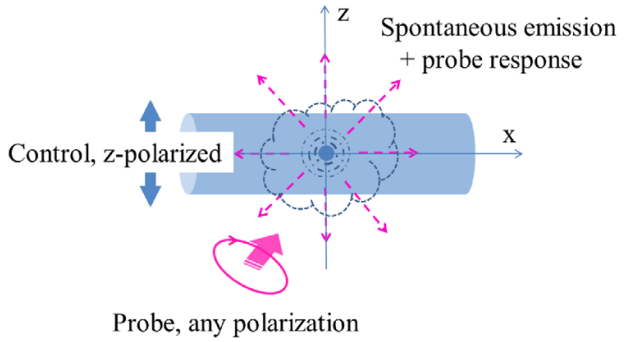

Fig. 2. Excitation geometry of an isolated atom, thinkable as an elementary scatterer inside a dilute atomic cloud, and driven by two modes of the strong control and weak probe, as shown in Fig. 1. The responding field contains both the spontaneous emission and scattered part of the probe mode.

where the longitudinal electric field component (second term in the first line) is given by Eq. (S1.27) in Section 1 of Supplement 1. By keeping only the first expectation values of (2.4), we arrive at the textbook layout for the macroscopic Maxwell equations of a dielectric medium.

However, in the model considered, only the wave-type equation for the transverse electric field is important and meaningful since (i) the magnetic field has no action on the atoms and (ii) the longitudinal field only copies the dynamics of the dipoles, i.e., their local response to the external field. From (2.1), we obtain

$$\Delta\hat{\mathbf{E}}_{\perp}(\mathbf{R},t)-\frac{1}{c^2}\ddot{\hat{\mathbf{E}}}_{\perp}(\mathbf{R},t)=\frac{4\pi}{c^2}\ddot{\hat{\mathbf{P}}}_{\perp}(\mathbf{R},t), \tag{2.6}$$

where the term on the right-hand side defines the time derivative of the transverse polarization current.

The Maxwell–Heisenberg equations are obviously incomplete. They should be considered together with complementary equations for the atomic subsystem. In a nonlinear regime, the problem is extremely hard even for relatively simple energy configurations. In this paper, we focus on the Mollow problem with the basic transition diagram shown in Fig. 1. The medium atom has a single non-degenerate ground state and three excited Zeeman sublevels, i.e., its energy structure is associated with the simplest ${}^1S_0\to{}^1P_1$ optical transition. It is driven by a strong quasi-resonance coherent field (further referred to as the control field), shown by the shaded arrow in the diagram, and, in a steady-state regime, has a nonlinear fluorescence response in three resonance lines known as Mollow triplet. The ensemble of such atoms constructs a disordered atomic medium, where a weak probe light can propagate along an arbitrary direction and with an arbitrary polarization. The latter can be superposed in three orthogonal components defined in the reference frame with its z-axis directed along the polarization vector of the strong control mode.

The suggested Maxwell–Heisenberg approach is generally applicable not only to a dilute gas but also to a highly dense system. However, as clarified in Section 1 of Supplement 1, the subtle structure of the system Hamiltonian in its interaction part, critically important for proximal dipoles, and physical duality in classification of the field variables inside the medium, namely, the difference between electric and displacement components, make the evaluation of the system's response on a weak probe quite challenging, particularly when the reference transitions are driven by the control field.

3. KUBO FORMULA FOR A DILUTE SYSTEM UNDER NONLINEAR EXCITATION

The dilute configuration usually allows us to make a crucial simplifying step in resolving the problem. In the dilute gas, where in the main spatial areas, unoccupied by particles, $\hat{\mathbf{D}}(\mathbf{R})\approx\hat{\mathbf{E}}_{\perp}(\mathbf{R})\approx\hat{\mathbf{E}}_{\rm tot}(\mathbf{R})$, so that the mutual interference of the proximal dipoles can be safely ignored, we can replace the displacement field by the transverse electric field in the interaction term. For a dilute atomic ensemble, the polarization current responding to the excitation scheme shown in Fig. 1 can be found in a closed form. In Fig. 2, we show the excitation geometry associated with the transition diagram of Fig. 1, which we will follow in our derivation.

A. Single Atom Response

As is common in the evaluation of a linear response to a weak probe associated with a specific quantized mode, we can select in the total Hamiltonian the interaction part with it as follows:

$$\hat{H}(t)=\hat{H}_0(t)-\hat{\mathbf{d}}\cdot\hat{\mathcal{E}}, \tag{3.1}$$

where we include in the operator $\hat{\mathcal{E}}$ only one specific probe (which we shall also refer to as signal) mode,

$$\hat{\mathcal{E}}(\mathbf{R})=\left(\frac{2\pi\hbar\omega}{V}\right)^{1/2}\left[i\mathbf{e}a\mathrm{e}^{+i\mathbf{k}\cdot\mathbf{R}}-i\mathbf{e}^{*}a^{\dagger}\mathrm{e}^{-i\mathbf{k}\cdot\mathbf{R}}\right], \tag{3.2}$$

where for the sake of notation simplicity and derivation clarity, we have omitted the index specification of this mode. It is a crucial assumption that elimination of only one mode, defined as $\{\mathbf{e},\,\omega=ck,\,\mathbf{k}\}$, from the complete continuum of field modes in Eq. (S1.7) in Section 1 of Supplement 1, does not affect the original system dynamics driven by the control field and its coupling with the resting part of the field continuum. The probe field contributes to (3.1) at the point of the dipole location $\hat{\mathcal{E}}\equiv\hat{\mathcal{E}}(\mathbf{R}=\mathbf{0})$.

Because of the action of the classical control field, the internal Hamiltonian $\hat{H}_0(t)$ depends on time even in the Schrödinger representation:

$$\hat{H}_0(t) = \hat{H}_{\text{Atom}} + \sum_s \hbar\omega_s (a_s^\dagger a_s + 1/2) - \frac{\hbar\Omega_R}{2}|b\rangle\langle a|e^{-i\omega_c t} - \frac{\hbar\Omega_R}{2}|a\rangle\langle b|e^{+i\omega_c t} - \hat{\mathbf{d}}\cdot\hat{\mathbf{E}}', \tag{3.3}$$

where ω_c is the frequency of the coherent control field, and we have implied the rotating wave approximation (RWA) for interaction with all the field modes distributed near the reference atomic optical transition with frequency $\omega_b \equiv \omega_0$; see definition of the atomic Hamiltonian in the Eq. (S1.2) of Supplement 1 (with its self-energy part neglected). Here $\hbar\Omega_R = d_0 E_0$ denotes the Rabi frequency Ω_R of the control field for coupling the states $|a\rangle = |0, 0\rangle$ and $|b\rangle = |1, 0\rangle$ (see Fig. 1), and $d_0 = d_{ab} = d_{ba} > 0$ is the matrix element of the transition dipole moment, which, without loss of generality is assumed to be real and positive. Because of free choice in definition of the initial time, we can assume $\Omega_R > 0$, i.e., fix the complex amplitude E_0 as real and positive as well. In the last term, responding for interaction with the quantized and initially unoccupied vacuum modes, we have eliminated the interaction with the control and probe modes. For clarity, the absence of these modes is superscribed by the prime sign $\hat{\mathbf{E}}'$ in the last term of (3.3), where the complete field operator $\hat{\mathbf{E}} \equiv \hat{\mathbf{E}}(\mathbf{R} = \mathbf{0})$ is given by expansion Eq. (S1.7) in Section 1 of Supplement 1.

Defining the evolutionary operator of the Hamiltonian (3.3)

$$U(t, 0) = T\exp\left[-\frac{i}{\hbar}\int_0^t \hat{H}_0(t')\mathrm{d}t'\right], \tag{3.4}$$

where T is the chronologically ordering operator acting on each operator product appearing from the exponent expansion: $\hat{H}_0(t_1)\hat{H}_0(t_2)\ldots\hat{H}_0(t_n)$, such that $t_1 > t_2 > \ldots > t_n$. Then, we can define the interaction representation for any system operator. In particular, the dipole moment transforms as follows:

$$\hat{\mathbf{d}}(t) = U^\dagger(t, 0)\hat{\mathbf{d}}U(t, 0). \tag{3.5}$$

In accordance with our above assumptions, we neglect those parts of the emitted nonlinear fluorescence, which would overlap the probe mode, and accept

$$\hat{\mathcal{E}}(\mathbf{R}, t) = U^\dagger(t, 0)\hat{\mathcal{E}}(\mathbf{R})U(t, 0), = \left(\frac{2\pi\hbar\omega}{V}\right)^{1/2}\left[i\mathbf{e}\ a(t)e^{+i\mathbf{k}\cdot\mathbf{R}} - i\mathbf{e}^* a^\dagger(t)e^{-i\mathbf{k}\cdot\mathbf{R}}\right], \equiv \left(\frac{2\pi\hbar\omega}{V}\right)^{1/2}\left[i\mathbf{e}\ a e^{-i\omega t+i\mathbf{k}\cdot\mathbf{R}} - i\mathbf{e}^* a^\dagger e^{+i\omega t-i\mathbf{k}\cdot\mathbf{R}}\right]. \tag{3.6}$$

These basic transformations allow us to express system dynamics in the interaction representation.

Indeed, the basic Schrödinger equation for an arbitrary system state $|t\rangle_S$ in the Schrödinger representation reads

$$i\hbar\frac{\partial}{\partial t}|t\rangle_S = \left[\hat{H}_0(t) - \hat{\mathbf{d}}\cdot\hat{\mathcal{E}}\right]|t\rangle_S. \tag{3.7}$$

By making use of (3.4), we can link it to the interaction representation

$$|t\rangle_S = U(t, 0)|t\rangle_I, \tag{3.8}$$

and construct the Schrödinger equation in the interaction representation

$$i\hbar\frac{\partial}{\partial t}|t\rangle_I = -\hat{\mathbf{d}}(t)\cdot\hat{\mathcal{E}}(t)|t\rangle_I, \tag{3.9}$$

where $\hat{\mathbf{d}}(t)$ and $\hat{\mathcal{E}}(t)$ are, respectively, given by (3.5) and (3.6).

We can completely eliminate the state dependence on time by introducing the evolutionary transformation from the interaction to the Heisenberg picture:

$$S(t, 0) = T\exp\left[+\frac{i}{\hbar}\int_0^t \hat{\mathbf{d}}(t')\cdot\hat{\mathcal{E}}(t')\mathrm{d}t'\right], \tag{3.10}$$

and

$$|t\rangle_I = S(t, 0)|\rangle_H \tag{3.11}$$

constitutes the time-independent state $|\rangle_H$ in the Heisenberg description of the system dynamics.

Eventually, the dipole operator in the Heisenberg representation is given by

$$\hat{\mathbf{d}}_H(t) = S^\dagger(t, 0)\hat{\mathbf{d}}(t)S(t, 0), \approx \hat{\mathbf{d}}(t) - \frac{i}{\hbar}\int_0^t \left[\hat{\mathbf{d}}(t')\cdot\hat{\mathcal{E}}(t'), \hat{\mathbf{d}}(t)\right]\mathrm{d}t' + \ldots, \tag{3.12}$$

where in the second line, we have implied the first-order approximation in the expansion of the evolutionary operator. For the sake of notation convenience, here we additionally subscribe this operator by "H" and reserve lighter notation $\hat{\mathbf{d}}(t)$ for the interaction dynamics, which is actually important for us and will be further tracked throughout our derivation.

The Kubo formula follows directly from (3.12), written in terms of expectation values, and assumes a given dipole position. Throughout our consideration, we treat the position of atom[s] classically. Thus, in order to link it with the dipole density, we have to multiply (3.12) by $\delta(\mathbf{R})$. The mean dipole density (local polarization) of a single atom is given by

$$\mathbf{P}(\mathbf{R}, t) = \langle\hat{\mathbf{d}}_H(t)\rangle\delta(\mathbf{R}) \equiv \bar{\mathbf{d}}_H(t)\delta(\mathbf{R}), \tag{3.13}$$

and the mean probe field

$$\mathcal{E}(\mathbf{R}, t) = \langle\hat{\mathcal{E}}(\mathbf{R}, t)\rangle. \tag{3.14}$$

Then (3.12) leads to

$$P_i(\mathbf{R}, t) = \bar{d}_i(t)\delta(\mathbf{R}) + \int_{-\infty}^t \alpha_{ij}(\mathbf{R}; t, t')\mathcal{E}_j(\mathbf{R}, t')\mathrm{d}t', \tag{3.15}$$

where

$$\alpha_{ij}(\mathbf{R}; t, t') = \frac{i}{\hbar}\left\langle\left[\hat{d}_i(t), \hat{d}_j(t')\right]\right\rangle\delta(\mathbf{R}) \tag{3.16}$$

defines the polarizability tensor for a single atom in the Cartesian basis with $i, j = x, y, z$ and with default sum in (3.15) over the repeated tensor index.

The relations (3.15) and (3.16), derived for a linear response of the dipole polarization on a probe mode, constitute the Kubo formula in the case of a single atom; see [23]. However, the presence of the first term in (3.15) is a consequence of the nonlinear dynamics of the atomic dipole driven by the Hamiltonian (3.3). In the steady state excitation condition, formally approached by $t \to \infty$, and in assumption that $\alpha_{ij}(\mathbf{R}; t, t') \to 0$ if $t - t' \to \infty$, the integral in (3.15) becomes independent of its lower time argument, formally extended to $-\infty$.

B. Generalization on a Multi-Particle System

For a multi-particle system, instead of (3.1), we have

$$\hat{H}(t) = \hat{H}_0(t) - \sum_{a=1}^{N} \hat{\mathbf{d}}^{(a)} \cdot \hat{\mathcal{E}}_a, \tag{3.17}$$

where $\hat{\mathcal{E}}_a$ is given by (3.2) at the point of a th atom location: $\hat{\mathcal{E}}_a \equiv \hat{\mathcal{E}}(\mathbf{R} = \mathbf{R}_a)$. The undisturbed Hamiltonian is given by

$$\begin{aligned}\hat{H}_0(t) = &\sum_{a=1}^{N} \hat{H}^{(a)}_{\text{Atom}} + \sum_{s} \hbar\omega_s (a_s^\dagger a_s + 1/2) \\ &- \sum_{a=1}^{N} \left[\frac{\hbar\Omega_R}{2} |b\rangle\langle a|^{(a)} \mathrm{e}^{-i\omega_c t + i\mathbf{k}_c\cdot\mathbf{R}_a} \right. \\ &\left. + \frac{\hbar\Omega_R}{2} |a\rangle\langle b|^{(a)} \mathrm{e}^{+i\omega_c t - i\mathbf{k}_c\cdot\mathbf{R}_a} \right] - \sum_{a=1}^{N} \hat{\mathbf{d}}^{(a)} \cdot \hat{\mathbf{E}}'(\mathbf{R}_a),\end{aligned} \tag{3.18}$$

where here and throughout, we superscribe by the atom's number its internal Hamiltonian and dyad-type operators. The critical aspect in Eq. (3.18) is the spatial dependence of the interaction terms for each particular atomic dipole.

The Rabi frequencies are changed along the sample, so that in general $\Omega_R = \Omega_R(\mathbf{R}_a)$. However, in dilute systems, the scattering and depletion of the control field are weak processes. That means that for sufficiently long distances inside the sample, it can be assumed to have a uniform profile. Its spatial dependence along the sample can be approximately taken into account by spatial parametrization of the sample susceptibility in the finally derived equations.

Other transformations are straightforward. The evolutionary operator $U(t, 0)$ is defined by (3.4) and transformation (3.5) should be specified for each dipole:

$$\hat{\mathbf{d}}^{(a)}(t) = U^\dagger(t, 0)\hat{\mathbf{d}}^{(a)}U(t, 0), \tag{3.19}$$

and (3.6) is unchanged. Equations (3.7)–(3.11) should be generalized for the collection of atoms, and $|t\rangle_S$, $|t\rangle_I$, and $|\rangle_H$ would describe the quantum states of the global system. The evolutionary operator (3.10), responsible for the interaction of the dipoles with the probe mode, generalizes as

$$S(t, 0) = T\exp\left[+\frac{i}{\hbar} \int_0^t \sum_{b=1}^{N} \hat{\mathbf{d}}^{(b)}(t') \cdot \hat{\mathcal{E}}_b(t') \mathrm{d}t' \right], \tag{3.20}$$

and instead of (3.12), we arrive at

$$\begin{aligned}\hat{\mathbf{d}}^{(a)}_H(t) &= S^\dagger(t, 0)\hat{\mathbf{d}}^{(a)}(t)S(t, 0) \\ &\approx \hat{\mathbf{d}}^{(a)}(t) - \frac{i}{\hbar} \sum_{b=1}^{N} \int_0^t \left[\hat{\mathbf{d}}^{(b)}(t') \cdot \hat{\mathcal{E}}_b(t'), \hat{\mathbf{d}}^{(a)}(t) \right] \mathrm{d}t' \\ &\quad + \dots\end{aligned} \tag{3.21}$$

The operators of atomic dipoles, dressed by interaction with the control field, are delocalized and share all the positions $a, b = 1, 2 \dots N$. The interaction of atoms with light, emitted as nonlinear fluorescence, can entangle them. In other words, the operators $\hat{\mathbf{d}}^{(b)}(t')$ and $\hat{\mathbf{d}}^{(a)}(t)$ for $a \neq b$ are generally uncommuted and correlated.

Equation (3.13) generalizes to

$$\mathbf{P}(\mathbf{R}, t) = \sum_{a=1}^{N} \langle \hat{\mathbf{d}}^{(a)}_H(t) \rangle \delta(\mathbf{R} - \mathbf{R}_a) \equiv \sum_{a=1}^{N} \bar{\mathbf{d}}^{(a)}_H(t) \delta(\mathbf{R} - \mathbf{R}_a), \tag{3.22}$$

and Eq. (3.21) leads to

$$\begin{aligned}P_i(\mathbf{R}, t) = &\sum_{a=1}^{N} \bar{d}^{(a)}_i(t) \delta(\mathbf{R} - \mathbf{R}_a) \\ &+ \int_{-\infty}^{t} \mathrm{d}t' \int \mathrm{d}^3 R' \alpha_{ij}(\mathbf{R}, t; \mathbf{R}', t') \mathcal{E}_j(\mathbf{R}', t'),\end{aligned} \tag{3.23}$$

where

$$\begin{aligned}&\alpha_{ij}(\mathbf{R}, t; \mathbf{R}', t') \\ &= \sum_{a,b} \alpha^{(a,b)}_{ij}(\mathbf{R}, t; \mathbf{R}', t'), \\ &\equiv \frac{i}{\hbar} \sum_{a,b} \left\langle \left[\hat{d}^{(a)}_i(t), \hat{d}^{(b)}_j(t') \right] \right\rangle \delta(\mathbf{R} - \mathbf{R}_a) \delta(\mathbf{R}' - \mathbf{R}_b),\end{aligned} \tag{3.24}$$

which shows, in general, a non-local response of the medium polarization on the weak driving probe, similar but not identical to the effect of spatial dispersion. The spatial correlations are created by the nonlinear dynamics of the dipoles and can exist only for a particular and frozen configuration of atoms.

C. Thermal Averaging

In reality, the positions of the atomic dipoles are random. Even if we consider an ensemble of cold atoms, so that the Doppler shifts are negligible, their spatial configuration is permanently changing. It is reasonable to assume that any interatomic correlations can be canceled out, and the dilute system celebrates the single atom response, expressed by (3.15) and (3.16):

$$P_i(\mathbf{R},t)=\bar{d}_i^{(\mathbf{R})}(t)n(\mathbf{R})+\int_{-\infty}^{t}\chi_{ij}(\mathbf{R};t,t')\mathcal{E}_j(\mathbf{R},t')\mathrm{d}t', \tag{3.25}$$

where

$$\chi_{ij}(\mathbf{R};t,t')=\frac{i}{\hbar}\left\langle\left[\hat{d}_i^{(\mathbf{R})}(t),\hat{d}_j^{(\mathbf{R})}(t')\right]\right\rangle n(\mathbf{R}) \tag{3.26}$$

is the medium dielectric susceptibility, if reduced per single atom, would be the same as a dipole polarizability $\alpha_{ij}(\mathbf{R};t,t')$. Here, $n=n(\mathbf{R})$ is a smoothed density distribution, expressed by a given uniform spatial profile, and the dipole $\hat{\mathbf{d}}^{(\mathbf{R})}(t)$ is driven by Hamiltonian (3.18) and is considered a function of the smoothed spatial coordinate $\mathbf{R}_a\to\mathbf{R}$.

4. SAMPLE SUSCEPTIBILITY IN CONDITIONS OF MOLLOW NONLINEAR EMISSION

The derived Kubo formula gives us a general mathematical resource to evaluate the sample susceptibility. However, this can be done only within certain assumptions, whose validity is provided by our model and clarified below.

A. Basic Definitions and Transformations

For an arbitrary atomic ensemble, the Hamiltonian (3.18) cannot be split into the sum of partial terms (3.3):

$$\hat{H}_0(t)\neq\sum_{a=1}^{N}\hat{H}_0^{(\mathbf{R})}(t)\Big|_{\mathbf{R}\to\mathbf{R}_a}, \tag{4.1}$$

because the field Hamiltonian is globally defined, and the quantized field exists as a unique undivided environment for all the atoms. The separation of proximal dipoles physically limits the scale for the quantization box in Eq. (S1.7) in Section 1 of Supplement 1, where it is assumed to be infinitely large.

For the term of interaction with the quantized field in (3.18), in assumption of the RWA approach, we can define

$$\begin{aligned}|b\rangle\langle b|&=|b\rangle\langle b|^{(\mathbf{R})},\\ |b\rangle\langle a|&=|b\rangle\langle a|^{(\mathbf{R})}\mathrm{e}^{+i\mathbf{k}_c\cdot\mathbf{R}},\\ |a\rangle\langle b|&=|a\rangle\langle b|^{(\mathbf{R})}\mathrm{e}^{-i\mathbf{k}_c\cdot\mathbf{R}},\end{aligned} \tag{4.2}$$

which shifts the frame origin to the atom's location.

We have arrived at an inconvenient observation: the operator transformations (4.2), aiming to boost the frame origin to a particular atom of the ensemble, map the dependence on its location on the field operators Eq. (S1.7) in Section 1 of Supplement 1. For a single atom it would not be a problem, since the extra phase shifts, induced in the field operators, can be incorporated into a fundamental phase uncertainty in the definition of the canonic operators a_s and $a_s^\dagger$. However, in a system consisting of many particles, the field modes should be specified as a unique set identical to either atom. We clearly see that the light–matter interaction is an intrinsically cooperative and configuration-dependent process. Hopefully, for a dilute atomic ensemble, the problem can be softened and resolved by the following arguments.

Imagine the atomic ensemble as loaded into a three-dimensional grid built up by physically scaled quantization boxes—$L\sim n_0^{-1/3}$—where n_0 is the density of atoms. Thus, on average, there is only one atom per each quantization box. The discretization of $\mathbf{k}$ by the quantization modes is now given by a "coarse-grained" scaling in the momentum space. The exponents in Eq. (S1.7) become periodic functions, whose argument gets maximal increment $k_xL+k_yL+k_zL \mod(2\pi)$ within each box. Additionally, we can fit the length L in such a way that the control field would also fulfill these revised quantization conditions. Then the meaningful variation of the exponent arguments in the interaction term of (3.18), estimated as $\sim\Delta\lambda/\lambda\, O(2\pi)\ll 1$, where $\Delta\lambda=\lambda-\lambda_c$ is a deviation of the wavelength justified by RWA, can be neglected.

We conclude that for any atom, taken from the ensemble, its dynamics is driven by the Hamiltonian (3.18), where the atom's location can be shifted to the frame origin while saving the uniform definition of the basic parameters such as Rabi frequency, transition dipole moments, etc. As a consequence, the Schrödinger precursors of its dyad operators (4.2) can evolve up to their Heisenberg dynamics being considered at the frame origin. Then, in the principal frame, with axes x,y,z (see Fig. 2), the commutator of the dipole operators in (3.26) can be expanded in terms of their frequency components as follows:

$$\left[\hat{d}_x^{(\mathbf{R})}(t),\hat{d}_x^{(\mathbf{R})}(t')\right]=\left[\hat{d}_x^{(+)}(t),\hat{d}_x^{(-)}(t')\right]+\left[\hat{d}_x^{(-)}(t),\hat{d}_x^{(+)}(t')\right], \tag{4.3}$$

$$\left[\hat{d}_y^{(\mathbf{R})}(t),\hat{d}_y^{(\mathbf{R})}(t')\right]=\left[\hat{d}_y^{(+)}(t),\hat{d}_y^{(-)}(t')\right]+\left[\hat{d}_y^{(-)}(t),\hat{d}_y^{(+)}(t')\right], \tag{4.4}$$

$$\begin{aligned}\left[\hat{d}_z^{(\mathbf{R})}(t),\hat{d}_z^{(\mathbf{R})}(t')\right]&=\left[\hat{d}_z^{(+)}(t),\hat{d}_z^{(-)}(t')\right]+\left[\hat{d}_z^{(-)}(t),\hat{d}_z^{(+)}(t')\right]\\&+\left[\hat{d}_z^{(+)}(t),\hat{d}_z^{(+)}(t')\right]\mathrm{e}^{+2i\mathbf{k}_c\cdot\mathbf{R}}+\left[\hat{d}_z^{(-)}(t),\hat{d}_z^{(-)}(t')\right]\mathrm{e}^{-2i\mathbf{k}_c\cdot\mathbf{R}},\end{aligned} \tag{4.5}$$

Here we have taken into account that the direct action of the control field does not concern the upper states $|1,\pm1\rangle$, and $\hat{d}_{x,y}(t)$ obey the dynamics, which is only indirectly affected by the coupling of the control field on $|a\rangle\to|b\rangle$ transition. Hence, the identical frequency components of $\hat{d}_x(t)=\hat{d}_x^{(+)}(t)+\hat{d}_x^{(-)}(t)$ and $\hat{d}_y(t)=\hat{d}_y^{(+)}(t)+\hat{d}_y^{(-)}(t)$ commute at any time.

Express the dipole operators by the dyad operators. On the active transition, we have

$$\begin{aligned}\hat{d}_z^{(+)}(t)&=d_0|a\rangle\langle b|(t),\\ \hat{d}_z^{(-)}(t)&=d_0|b\rangle\langle a|(t),\end{aligned} \tag{4.6}$$

where the dynamics of the operators on the right-hand side can be found from the solution of the Mollow problem within its two-level approximation. Next, define the following two undisturbed upper states:

$$\begin{aligned}|x\rangle&\equiv\frac{1}{\sqrt{2}}\left[|1,-1\rangle-|1,+1\rangle\right]\to\frac{1}{2}\sqrt{\frac{3}{\pi}}\sin\theta\cos\phi,\\ |y\rangle&\equiv\frac{i}{\sqrt{2}}\left[|1,-1\rangle+|1,+1\rangle\right]\to\frac{1}{2}\sqrt{\frac{3}{\pi}}\sin\theta\sin\phi,\end{aligned} \tag{4.7}$$

which, together with the state

$$|b\rangle \equiv |z\rangle \to \frac{1}{2}\sqrt{\frac{3}{\pi}}\cos\theta \tag{4.8}$$

span the three-dimensional upper-level subspace onto a vector extension of the Mollow problem. Here θ, ϕ is the spherical angle, associated with the frame of Fig. 2, and $d_{ab} \equiv d_{az} = d_{ax} = d_{ay} = d_0 > 0$. Then, similar to (4.6), we define

$$\hat{d}_x^{(+)}(t) = d_0|a\rangle\langle x|(t),$$
$$\hat{d}_x^{(-)}(t) = d_0|x\rangle\langle a|(t), \tag{4.9}$$

$$\hat{d}_y^{(+)}(t) = d_0|a\rangle\langle y|(t),$$
$$\hat{d}_y^{(-)}(t) = d_0|y\rangle\langle a|(t). \tag{4.10}$$

The operators on the right-hand sides of (4.9) and (4.10) can be found via the solution of the extended Mollow problem, which we discuss in the next section.

B. Three-Dimensional Extension of the Mollow Problem

We follow and generalize the calculation approach of [24]. Let us define the following slow varying in time operators for the atom

$$\hat{\sigma}_+(t) = |b\rangle\langle a|(t)\mathrm{e}^{-i\omega_c t},$$
$$\hat{\sigma}_-(t) = |a\rangle\langle b|(t)\mathrm{e}^{+i\omega_c t},$$
$$\hat{\sigma}_Z(t) = \frac{1}{2}[|b\rangle\langle b|(t) - |a\rangle\langle a|(t)], \tag{4.11}$$

where the lower sign indices $_\pm$, associated with either rising or lowering excitation, should not be confused with the upper indices $^{(\pm)}$, associated with the operator's frequency components, and the capital Z-index, specifying the atomic pseudospin, should not be confused with the vector component z.

Then, for the main excitation channel $|a\rangle \to |b\rangle$ the Heisenberg–Langevin dynamical equations for the atomic operators subsequently read:

$$\dot{\hat{\sigma}}_+(t) = \left(-\mathrm{i}\Delta - \frac{\gamma}{2}\right)\hat{\sigma}_+(t) + \mathrm{i}\Omega_R\hat{\sigma}_Z(t) + \hat{F}_+(t),$$
$$\dot{\hat{\sigma}}_-(t) = \left(+\mathrm{i}\Delta - \frac{\gamma}{2}\right)\hat{\sigma}_-(t) - \mathrm{i}\Omega_R\hat{\sigma}_Z(t) + \hat{F}_-(t),$$
$$\dot{\hat{\sigma}}_Z(t) = \mathrm{i}\frac{\Omega_R}{2}\left[\hat{\sigma}_+(t) - \hat{\sigma}_-(t)\right] - \gamma\left[\hat{\sigma}_Z(t) + \frac{1}{2}\right] + \hat{F}_Z(t), \tag{4.12}$$

where $\Delta = \omega_c - \omega_0$, and γ is the natural decay rate of the atomic excited state. The noise terms are given by

$$\hat{F}_+(t) = +2\mathrm{i}\frac{d_0}{\hbar}\hat{E}_{0z}^{(-)}(t)\mathrm{e}^{-\mathrm{i}\omega_c t}\hat{\sigma}_Z(t),$$
$$\hat{F}_-(t) = -2\mathrm{i}\frac{d_0}{\hbar}\hat{\sigma}_Z(t)\hat{E}_{0z}^{(+)}(t)\mathrm{e}^{+\mathrm{i}\omega_c t},$$
$$\hat{F}_Z(t) = +\mathrm{i}\frac{d_0}{\hbar}\left[\hat{\sigma}_+(t)\hat{E}_{0z}^{(+)}(t)\mathrm{e}^{+\mathrm{i}\omega_c t} - \hat{E}_{0z}^{(-)}(t)\mathrm{e}^{-\mathrm{i}\omega t}\hat{\sigma}_-(t)\right], \tag{4.13}$$

where the field operators $\hat{E}_{0z}^{(\pm)}(t)$ are freely evolving Heisenberg images of the operators Eq. (S1.7) in Section 1 of Supplement 1. These equations are close-coupled but insufficient for a three-dimensional description.

The weak excitation by the probe mode also concerns the satellite transitions $|a\rangle \to |x\rangle$ and $|a\rangle \to |y\rangle$, which evolve independently. They are similarly described and further we only follow the disturbed Heisenberg dynamics of rising/lowering operators for $|a\rangle \to |x\rangle$ channel:

$$\hat{\sigma}_+^{(x)}(t) = |x\rangle\langle a|(t)\mathrm{e}^{-i\omega_c t},$$
$$\hat{\sigma}_-^{(x)}(t) = |a\rangle\langle x|(t)\mathrm{e}^{+i\omega_c t}. \tag{4.14}$$

The dynamics of $\hat{\sigma}_+^{(x)}(t)$ obey the following two coupled equations:

$$\dot{\hat{\sigma}}_+^{(x)}(t) = \left(-\mathrm{i}\Delta - \frac{\gamma}{2}\right)\hat{\sigma}_+^{(x)}(t) + \frac{\mathrm{i}}{2}\Omega_R|x\rangle\langle b|(t) + \hat{F}_+^{(x)}(t),$$
$$\frac{\partial}{\partial t}|x\rangle\langle b|(t) = -\gamma|x\rangle\langle b|(t) + \frac{\mathrm{i}}{2}\Omega_R\hat{\sigma}_+^{(x)}(t) + \hat{F}^{(xb)}(t), \tag{4.15}$$

with the noise terms given by

$$\hat{F}_+^{(x)}(t) = \mathrm{i}\frac{d_0}{\hbar}\hat{E}_{0z}^{(-)}(t)|x\rangle\langle b|(t)\mathrm{e}^{-\mathrm{i}\omega_c t} + \mathrm{i}\frac{d_0}{\hbar}\hat{E}_{0x}^{(-)}(t)\mathrm{e}^{-\mathrm{i}\omega_c t}[|x\rangle\langle x|(t) - |a\rangle\langle a|(t)],$$
$$\hat{F}^{(xb)}(t) = +\mathrm{i}\frac{d_0}{\hbar}\left[\hat{\sigma}_+^{(x)}(t)\hat{E}_{0z}^{(+)}(t)\mathrm{e}^{+\mathrm{i}\omega_c t} - \hat{E}_{0x}^{(-)}(t)\mathrm{e}^{-\mathrm{i}\omega_c t}\hat{\sigma}_-(t)\right]. \tag{4.16}$$

For the conjugated operator $\hat{\sigma}_-^{(x)}(t)$, the dynamics is driven by the equations Hermitian conjugated to (4.15) and (4.16).

The closed-coupled Eqs. (4.12) and (4.13) are solved independently. But its solution further strongly affects the solution of Eqs. (4.15) and (4.16) and is expressed in the dynamics of $\hat{\sigma}_\pm^{(x)}(t)$. That is a direct consequence of the fact that the system, being physically driven by the Hamiltonian (3.3), activates not only the occupied states but the operator dynamics existing at the level of quantum fluctuations as well. Note that all these equations would simplify and become independent once the control field vanishes $\Omega_R \to 0$.

1. Subject of Calculation

It is sufficient to evaluate only the positive frequency response of the susceptibility tensor (3.26), which can be selected from the commutator expansions (4.3)–(4.5). In the steady-state regime

for the dipole's response on a probe, polarized along principal axis x, such a component is given by

$$\chi_{xx}^{(+)}(\tau) = \frac{i}{\hbar} n_0 d_0^2 \left\langle \left[\hat{\sigma}_-^{(x)}(t), \hat{\sigma}_+^{(x)}(t-\tau) \right] \right\rangle e^{-i\omega_c \tau}, \quad \textbf{(4.17)}$$

being independent on observation time t. Here, without loss of generality, we have assumed an infinite homogeneous medium with density n_0, and recall the comment after (3.18).

However the dipole's response on a probe, polarized along the z-direction, is more tricky and consists of two contributions:

$$\chi_{zz}^{(+)}(t, t') = \chi_{zz}^{(+-)}(t-t') + \chi_{zz}^{(++)}(t, t') e^{+2i\mathbf{k}_c \cdot \mathbf{R}}, \quad \textbf{(4.18)}$$

where the first term expresses the dynamics of the atomic dipole driven by the positive frequency component of the probe mode. Similar to (4.17), it is given by

$$\chi_{zz}^{(+-)}(\tau) = \frac{i}{\hbar} n_0 d_0^2 \left\langle \left[\delta\hat{\sigma}_-(t), \delta\hat{\sigma}_+(t-\tau) \right] \right\rangle e^{-i\omega_c \tau}, \quad \textbf{(4.19)}$$

where for the sake of further derivation convenience, we have subtracted the mean expectation values of the operator functions and defined $\delta\hat{\sigma}_\pm(t) = \hat{\sigma}_\pm(t) - \bar{\sigma}_\pm(t)$. The second term expresses the parametric response of the positive component driven by the negative frequency component of the probe:

$$\chi_{zz}^{(++)}(t, t')\big|_{t'=t-\tau} = \frac{i}{\hbar} n_0 d_0^2 \left\langle \left[\delta\hat{\sigma}_-(t), \delta\hat{\sigma}_-(t-\tau) \right] \right\rangle e^{-i\omega_c (t+t')}, \quad \textbf{(4.20)}$$

where the expectation value of the commutator is independent of the observation time t.

In the steady-state regime, the susceptibility tensor is defined by the Fourier transformation of the above functions to the frequency representation. In the case considered, the spectral components are distributed in a vicinity of the reference frequencies $\omega \sim \omega_c, \omega_0$. Then we can parameterize the Fourier images by detuning $\Omega = \omega - \omega_c$ and apply it to the slow varying functions of τ contributing in (4.18)–(4.20).

Omit the trivial multiplication factors as well as the exponents, structuring the spatial and temporal phase matching conditions, and define the following principal components of the susceptibility tensor:

$$\chi_{xx}^{(+)}(\Omega) \propto \int_0^\infty d\tau e^{+i\Omega\tau} \left\langle \left[\hat{\sigma}_-^{(x)}(t), \hat{\sigma}_+^{(x)}(t-\tau) \right] \right\rangle, \quad \textbf{(4.21)}$$

$$\chi_{zz}^{(+-)}(\Omega) \propto \int_0^\infty d\tau e^{+i\Omega\tau} \left\langle \left[\delta\hat{\sigma}_-(t), \delta\hat{\sigma}_+(t-\tau) \right] \right\rangle, \quad \textbf{(4.22)}$$

$$\chi_{zz}^{(++)}(\Omega) \propto \int_0^\infty d\tau e^{-i\Omega\tau} \left\langle \left[\delta\hat{\sigma}_-(t), \delta\hat{\sigma}_-(t-\tau) \right] \right\rangle, \quad \textbf{(4.23)}$$

where we have paid attention to the fact that the retardation in (3.25) dictates that $\tau > 0$.

Although the transformations (4.21)–(4.23) look similar, there is an important difference in physics between them. The susceptibilities (4.21) and (4.22) are the elastic response to the probe mode $\omega = \omega_c + \Omega$, involved in the Rayleigh or stimulated quasi-Raman processes. In the latter case, the probe light is reconverted by stimulated scattering into the control mode and back to the probe. This type of coherent response is quite similar to those normally developing in an undisturbed dielectric medium. The critical difference is that in the nonlinear medium, the probe experiences the quasi-energy structure created by the control field. The susceptibility (4.23) expresses a specific phase-sensitive nonlinear process, namely, the parametric conversion of the signal probe mode $\omega = \omega_s = \omega_c + \Omega$ to another idler probe mode $\omega_i = \omega_c - \Omega$. The spatial exponent in (4.18) provides this process to expand primary under the spatial phase matching conditions with $2\mathbf{k}_c \approx \mathbf{k}_s + \mathbf{k}_i$. That is fulfilled only approximately in an inhomogeneous sample.

We can explain our calculation algorithm of (4.21)–(4.23) in an example of the z-polarized probe. Define the generalized Fourier transform for the operator fluctuations:

$$\delta\hat{\sigma}_-(\Omega) = \int_{-\frac{T}{2}}^{\frac{T}{2}} dt\, e^{i\Omega t} \delta\hat{\sigma}_-(t),$$

$$\delta\hat{\sigma}_+(\Omega) = \int_{-\frac{T}{2}}^{\frac{T}{2}} dt\, e^{i\Omega t} \delta\hat{\sigma}_+(t) = \delta\hat{\sigma}_-^\dagger(-\Omega),$$

$$\delta\hat{\sigma}_Z(\Omega) = \int_{-\frac{T}{2}}^{\frac{T}{2}} dt\, e^{i\Omega t} \delta\hat{\sigma}_Z(t), \quad \textbf{(4.24)}$$

which are parameterized by infinitely long $T \to +\infty$ and obey the periodic boundary conditions. This transforms Eq. (4.12) into algebraic and analytically solvable equations. Then we make use of identities:

$$\int_{-\infty}^{\infty} d\tau e^{+i\Omega\tau} \left\langle \left[\delta\hat{\sigma}_-(t), \delta\hat{\sigma}_+(t-\tau) \right] \right\rangle = \lim_{T\to\infty} \frac{1}{T} \left\langle \left[\delta\hat{\sigma}_-(\Omega), \delta\hat{\sigma}_+(-\Omega) \right] \right\rangle, \quad \textbf{(4.25)}$$

$$\int_{-\infty}^{\infty} d\tau e^{-i\Omega\tau} \left\langle \left[\delta\hat{\sigma}_-(t), \delta\hat{\sigma}_-(t-\tau) \right] \right\rangle = \lim_{T\to\infty} \frac{1}{T} \left\langle \left[\delta\hat{\sigma}_-(-\Omega), \delta\hat{\sigma}_-(\Omega) \right] \right\rangle. \quad \textbf{(4.26)}$$

That lets us construct the spectral expansion of the correlation functions (expectation values of the commutators in the frequency representation), formally containing both the retarded ($\tau > 0$) and advanced ($\tau < 0$) branches, and express them via correlation functions of the Langevin sources (4.13), which we clarify below.

The retarded branch can be recovered by the following convolution transform of the Fourier images:

$$\int_0^\infty d\tau e^{\pm i\Omega\tau} f(\tau) = i \int_{-\infty}^{+\infty} \frac{d\Omega'}{2\pi} \frac{F[f](\Omega')}{\pm\Omega - \Omega' + i0}, \quad \textbf{(4.27)}$$

where $F[f](\Omega')$ is the Fourier image of $f(\tau)$ in conventional form, i.e.,

$$F[f](\Omega') = \int_{-\infty}^{+\infty} d\tau e^{+i\Omega'\tau} f(\tau). \quad \textbf{(4.28)}$$

The integral on the right-hand side can be looped by a contour in any half-plane of the complex-valued Ω' and expressed by the sum of the residues of the integrand inside the contour.

2. Correlation Properties of the Noise Sources

The described algorithm is crucially based on knowledge of the correlation properties of the noise terms. For Eq. (4.12) the noise sources (4.13) fulfill the following symmetry relations:

$$\hat{F}_+^\dagger(t) = \hat{F}_-(t), \quad \hat{F}_Z^\dagger(t) = \hat{F}_Z(t), \tag{4.29}$$

and their correlations are relevantly approximated by delta-correlated Wiener-type random processes with

$$\left\langle \hat{F}_q^\dagger(t)\hat{F}_{q'}(t')\right\rangle = 2D_{qq'}\delta(t-t'), \tag{4.30}$$

where the diffusion coefficients can be structured in the following matrix:

$$D_{qq'} = \frac{\gamma}{2}\begin{pmatrix} 1 & 0 & \langle\hat{\sigma}_-(t)\rangle \\ 0 & 0 & 0 \\ \langle\hat{\sigma}_+(t)\rangle & 0 & 1/2+\langle\hat{\sigma}_Z(t)\rangle \end{pmatrix}, \tag{4.31}$$

with matrix raw/column ordered as $q, q' = +, -, Z$. This matrix is assumed to be independent of time in the steady-state excitation regime. Then the mean values of $\langle\hat{\sigma}_\pm(t)\rangle$ and $\langle\hat{\sigma}_Z(t)\rangle$ are given by a stationary solution of the optical Bloch equations.

For Eqs. (4.15), (4.16), and for their Hermitian counterparts, we can order the correlation properties in form (4.30) with the following matrix of diffusion coefficients:

$$D_{qq'} = \frac{\gamma}{2}\begin{pmatrix} 1 & 0 & \langle\hat{\sigma}_-(t)\rangle & 0 \\ 0 & 0 & 0 & 0 \\ \langle\hat{\sigma}_+(t)\rangle & 0 & 1/2+\langle\hat{\sigma}_Z(t)\rangle & 0 \\ 0 & 0 & 0 & 0 \end{pmatrix}, \tag{4.32}$$

where $q, q' = {}^{(x)}_{+}, {}^{(x)}_{-}, {}^{(xb)}, {}^{(bx)}$.

By concluding this section, let us make one remark concerning the general description of the parametric process. Actually, the developed approach includes an optical nonlinearity incorporating all accessible orders of wave mixing with respect to the control field. The higher orders of nonlinearity reveal themselves in the self-conversion of the control mode in this process. Since we have studied such a nonlinear medium, disturbed by a single mode of a weak signal light, the process generates only one phase-conjugated idler response to it. We have neglected any higher-order nonlinearities associated with the signal light, which are excluded by our basic relation (3.25). However, in spontaneous parametric scattering, considered from a single atomic emitter, all the orders of the wave mixing could be accessible. Nevertheless, for light emission collected from a mesoscopically scaled atomic volume consisting of many atoms, the higher orders are expected to be weakened because of Gaussian factorization of the field correlation functions of higher orders, with a dominating contribution from the four-wave mixing process. The latter is governed by the parametric part of the nonlinear susceptibility (4.23).

5. RESULTS FOR A DILUTE SYSTEM

The solution of (4.12) and (4.15) is detailed in Section 2 of Supplement 1, and, in its general case, can be finalized only numerically. Here we present the principal components of the susceptibility tensor, calculated for different saturation parameters s, defined by Eq. (S2.2), and for $\Delta = 0$, i.e., for the control field resonant to the reference atomic transition. The susceptibility components (4.21)–(4.23), given by the integral expansions (S2.5)–(S2.7), are further scaled by a dimensionless factor expressed by the atomic density as

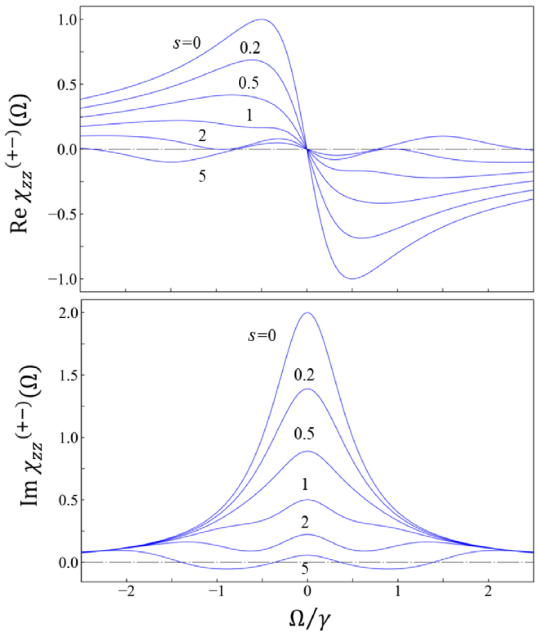

Fig. 3. Kerr-type nonlinear susceptibility for z-polarized probe (4.22), calculated for the control field resonant to the atomic transition, and for different saturation parameters s.

$$\frac{n_0 d_0^2}{\hbar\gamma} = n_0\frac{3c^3}{4\omega_0^3} \equiv \frac{3}{4}n_0\lambda\!\!\!^{-3}_0, \tag{5.1}$$

which for a dilute gas is a small quantity.

In Figs. 3 and 4, we show the parts of the susceptibilily tensor responsible for the stimulated scattering and spontaneous losses of the probe modes, polarized, respectively, along the z and x directions. As pointed above, these processes are initiated by Rayleigh and Raman-type scattering on the quasi-energy structure, distorted by the control field. Under the vision of macroscopic Maxwell theory, such a medium response can be associated with the polarization current activated by the probe mode. In these processes, the positive frequency component of the polarization (transition) current is driven by the same positive frequency component of the probe. We shall refer to it as a general Kerr-type optical nonlinearity, where the conventional dielectric properties of the atomic medium are modified by the action of a strong control field.

As follows from the dependencies of Fig. 3, the susceptibility of the z-polarized probe vanishes in the saturation limit when $s \gg 1$. However, the saturation regime is accompanied by a non-negligible manifestation of the negatively-valued imaginary part of the sample susceptibility, leading to enhancement of the propagating light. That is a certain consequence for the probe light to be partly amplified by the spontaneous emission from the Mollow sidebands. Such an amplification mechanism can be utilized in an optically dense gas for the preparation

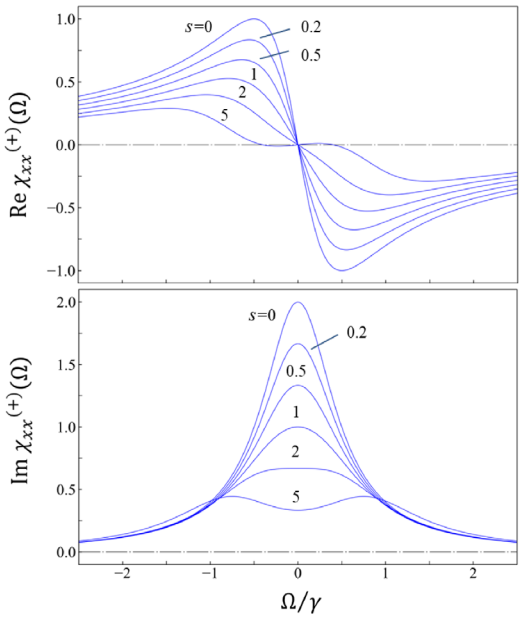

Fig. 4. Same as in Fig. 3 but for the x-polarized probe (4.21).

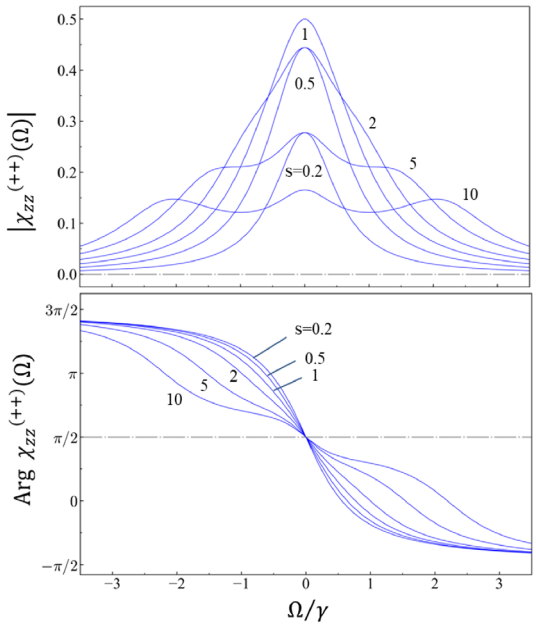

Fig. 5. Parametric nonlinear susceptibility (4.23), calculated for the control field resonant to the atomic transition, and for different saturation parameters s. The upper and lower plots, respectively, show its absolute value and argument.

conditions of a random laser generation, as proposed earlier in [22].

The susceptibility component responding to the x-polarized probe does not vanish with enlarging s but transforms to a doublet resonance structure, where the resonance maxima indicate the ac-Stark splitting of the ground state. As clarified in Section 2 of Supplement 1 in the saturation regime, the atoms populate the ground state with one-half probability and experience the Autler–Townes splitting observable by the sample probe on the adjacent transitions in either x or y polarizations. A signature of the Autler–Townes resonance structure for $s \gg 1$ is foreseen from the dependencies in Fig. 4.

The parametric coupling of the phase-conjugated probe modes, conventionally referred to as signal and idler, gives another type of nonlinearity. Let us focus on the optimal conditions for a maximally effective parametric amplification. The key feature of parametric nonlinearity is that the atomic medium is excluded from the energy interchange between the pump, signal, and idler modes. In other words, there are no energy losses in this interchange and the complexity of $\chi_{zz}^{(++)}(\Omega)$ indicates only the phase sensitivity of the parametric process. Unlike Figs. 3 and 4, instead of the real and imaginary parts, in Fig. 5, we show the absolute value and complex argument of the parametric nonlinear susceptibility responsible for the coupling of the phase-conjugated probe modes. This complex-valued quantity defines the coupling strength in an effective Hamiltonian governed by the joint dynamics of these modes under ideal conditions; see the comment ending Section 4.

The dependencies in the plots of Fig. 5 show that the efficiency of the parametric process cannot be infinitely enlarged if the pump becomes stronger. As follows from the calculated data, there is an optimal regime when the coupling strength is maximized near the intermediate saturation $s \sim 1$. For higher s the spectrum becomes broader with the Mollow sidebands are manifested. A local enhancement of the parametric coupling is observable near these sidebands.

6. INTERPOLATION TO A HIGH DENSITY

Let $\hat{T}^{(a)}$ be an arbitrary dyad-type operator associated with internal variables of an ath atom of the atomic subsystem, introduced in Section 4. In the general case, its Heisenberg dynamics obeys the following equation:

$$\dot{\hat{T}}^{(a)}(t) = \frac{i}{\hbar}\left[\hat{H}_{\rm Atom}^{(a)\prime}(t),\ \hat{T}^{(a)}(t)\right] - \frac{i}{\hbar}\left[\hat{d}_j^{(a)}(t),\ \hat{T}^{(a)}(t)\right] \times \frac{4\pi}{V}\sum_{b\neq a}^{N}{}' \sum_s e_{sj}\left(\mathbf{e}_s\cdot\hat{\mathbf{d}}^{(b)}(t)\right) e^{i\mathbf{k}_s\cdot(\mathbf{R}_a-\mathbf{R}_b)} - \frac{i}{\hbar}\hat{E}_{\perp j}^{(-)}(\mathbf{R}_a,t)\left[\hat{d}_j^{(a)}(t),\ \hat{T}^{(a)}(t)\right] - \frac{i}{\hbar}\left[\hat{d}_j^{(a)}(t),\ \hat{T}^{(a)}(t)\right]\hat{E}_{\perp j}^{(+)}(\mathbf{R}_a,t), \tag{6.1}$$

where the structure of the atom-field interaction is clarified in Section 1 of Supplement 1. The mode polarizations of the field vectors are defined in the Cartesian basis, and the default sum over repeated vector indices is assumed.

By substituting the microscopic displacement field, responsible for the atom-field coupling in the dipole gauge (see Section 1 of Supplement 1), into the interaction term, we have omitted the divergent contribution of the self-contact interaction. It is not a voluntary derivation step, but, as shown in [25], its action on the dipole dynamics is compensated by counteraction from the self-energy term contributed to the

atomic Hamiltonian; see Eqs. (S1.2)–(S1.4). So, the latter is also omitted in the atomic Hamiltonian of the particularly selected ath atom, and this circumstance is marked by the prime sign in (6.1).

The field variables contribute to Eq. (6.1) through the operators of the transverse electric field expanded in its positive and negative frequency components:

$$\hat{\mathbf{E}}_{\perp}(\mathbf{R},t)=\hat{\mathbf{E}}_{\perp}^{(+)}(\mathbf{R},t)+\hat{\mathbf{E}}_{\perp}^{(-)}(\mathbf{R},t) \tag{6.2}$$

taken at the point $\mathbf{R}=\mathbf{R}_a$ with running $a=1\ldots N$, where N is the number of atoms. As commented in Section 1 of Supplement 1, these operators do not commute with the atomic variables, and we have ordered them normally in Eq. (6.1). There is no need in such an ordering for the dipole operators $\hat{\mathbf{d}}^{(b)}(t)$ since for $b\neq a$ and at coincident moments of time they always commute with $\hat{T}^{(a)}(t)$.

The operators (6.2) fulfill the wave Eq. (2.6), being a direct consequence of the Heisenberg–Maxwell Eqs. (2.1) or (2.4). In (2.6), the atomic subsystem affects the field dynamics via the collective polarization current, which is contributed to the right-hand side of (2.6). Thus, considered together, (6.2) and (2.6) give us a close-coupled system of the Heisenberg equations, describing the joint dynamics of the atoms and field in arbitrary external conditions and for any medium densities consistent with the validity of the dipole long-wavelength approximation.

An issue naturally arises: can the system of Eqs. (2.6) and (6.1) be statistically averaged and expressed by the conventional form of the macroscopic Maxwell equations written for the mean field and mean dipole polarization? If the atomic medium is dense and excited by a strong external coherent field, the answer is probably negative. That is because the Mollow nonlinear fluorescence would be emitted by the medium atoms in arbitrary directions and would interfere with an external probe mode and create large fluctuations of the local field amplitude. An attempt was made to describe the interference of such random waves created by a coherent excitation in the saturation regime, specifically for a backward-scattering channel, in [16,17]. The damaging role of fluctuations on coherent processes of light propagation through a disordered ultracold atomic gas has been observed in experiments [14,15,18].

In the considered case, if the coherent pump is as strong as it saturates the $|a\rangle\leftrightarrow|b\rangle$ optical transition, such field fluctuations can withdraw the option of four-wave mixing and parametric amplification. Nevertheless, the situation can be improved if the external coherent field is not extremely strong and induces relatively weak nonlinear disturbances to the system. Then, at zero approximation, Eqs. (6.1) and (2.6) could be considered in the linear regime, and their correction by nonlinear dynamics could be taken into account as a perturbation to the light propagation process. In such an approximation, the second term in (6.1) reveals a local Lorentz–Lorenz correction to the electric field added by proximal dipoles, and the linear permittivity of the medium can be recovered by construction of a self-consistent functional equation [25]. Its solution at the high-density limit $n_0\lambda\!\!\!^{-3}_0\gg 1$ shows a nontrivial spectral behavior in the vicinity of the atomic resonance. The permittivity can be negative, so that the bulk atomic medium would have a forbidden zone preventing the penetration of a probe light inside the sample.

Apparently, the parametric process can evolve in the spectral domain, where the medium possesses normal dielectric properties with a real-valued dielectric constant $\varepsilon\sim\varepsilon'>1$, having a vanishing imaginary part $\varepsilon''\to 0$. As shown in [25], in such a spectral domain, the radiation decay should be renormalized as $\gamma\to\gamma_\varepsilon=\sqrt{\epsilon}\gamma$. Any atomic dipole, existing as an exciton-type quasiparticle, would obey the dynamics similar to that described in Section 4, where the transverse electric field of the probe light, acting on the dipole, would be displaced by the Lorentz–Lorenz correction to the local field.

Thus we can see that the single atom response to a signal mode, constructed in Section 2 of Supplement 1, is applicable for a dense atomic medium if (i) the control field is detuned to the spectral domain, where the medium is transparent, (ii) the decay rate γ is replaced by the renormalized decay constant γ_ε, and (iii) the solution, applied to a particular dipole, should be treated as a response on the local electric field. In such conditions, there is no physical resource for the parametric part of the susceptibility tensor to be significantly magnified by manipulating both the coherent pump and the sample density. In the considered model, the upper estimate for it cannot exceed the level of linear susceptibility of the sample in its transparency domain.

7. CONCLUSION

In this paper, we have attempted to follow a rigorous microscopic description of the macroscopic phenomenon of optical nonlinearity. For this, we have taken an example of a dense atomic ensemble consisting of neutral atoms interacting with an external electromagnetic field on a closed optical transition and framed our consideration by the long-wavelength dipole gauge. Although such a model deals with a rather simple matter object, it lets us enter to a more or less realistic physical visualization of a bulk medium, where the static interaction of proximal atomic dipoles interferes with their collective response to the transverse electric field, propagating through the medium and being dressed by interaction with it. We were motivated to clarify whether there are any internal barriers in such an atomic medium that would prevent an unlimited magnification of optical nonlinear susceptibility.

In a low-density limit, for a dilute configuration, the system's response to a weak probe field is correctly described by the generalized Kubo formula, where the nonlinear action of the strong control field is incorporated into the system's steady-state Heisenberg–Langevin dynamics. Each atomic dipole transforms into a Mollow-type quasiparticle, and a weak thermal disturbance converts the microscopic dynamics to the relevance of an average response of polarization current from mesoscopically scaled volumes of matter.

The derived expression for the susceptibility tensor is naturally divided into a sum of the Kerr-type and parametric nonlinearities, the latter being highlighted by the phase-matching conditions. We have obtained that in the saturation regime, the coherent processes are suppressed and, as a consequence, the parametric response, induced by four-wave mixing of the pump (control) and signal (probe), has a maximum as a function of the saturation parameter s near the point $s\sim 1$. In the saturation regime for large $s\gg 1$, the parametric

response tends to be redistributed to the vicinities of the Mollow sidebands.

It might be expected that the higher density of atoms would enhance the average mesoscopic polarization current and the parametric response, in particular. However, the joint manifestation of the nonlinearity and density effects dramatically complicates the physical picture and makes the macroscopic description problematic. As pointed out in Section 6, the randomly distributed Mollow nonlinear emission induces large fluctuations in the local electric field and breaks the justification for a macroscopic description in terms of the mean electric and displacement fields. In this case, we have foreseen only the option to drive the dielectric medium by a relatively weak control field in those spectral domains where the medium is transparent. In this case, the solution, originally obtained for a dilute configuration, could be renormalized and then would be applicable to a dense medium as well.

Finally, we have obtained, as a key result, that the internal interactions and the excitation by a strong control field, taken as a joint effect, mainly modify the quasi-energy structure of the atomic medium and cannot significantly magnify the coherent response of the polarization current to the driving fields. This can limit potential capabilities of quantum communication protocols, utilizing entangled photon pairs created by a parametric process as a main resource of quantum correlations. As we think, these statements can be generalized and applicable to other bulk media, where interaction with the external field is provided by a polarization current localized in a mesoscopically scaled volume. In particular, referring to the security level of quantum communication protocols, the discussed physical bounds could limit potential interference with an eavesdropper, in their exploiting the entangled photon pairs to attack a quantum channel utilizing a two-photon or multi-photon component of the coherent field for quantum key distribution.

Funding. Russian Science Foundation (23-72-10012); State Atomic Energy Corporation ROSATOM (868-1.3-15/15-2021, P2154); Foundation for the Advancement of Theoretical Physics and Mathematics (23-1-2-37-1 (BASIS)).

Disclosures. The authors declare no conflicts of interest.

Data availability. Data underlying the results presented in this paper are not publicly available at this time but may be obtained from the authors upon reasonable request.

Supplemental document. See Supplement 1 for supporting content.

REFERENCES

1. N. Lütkenhaus and M. Jahma, "Quantum key distribution with realistic states: photon-number statistics in the photon-number splitting attack," New J. Phys. **4**, 44 (2002).
2. J.-P. Chen, C. Zhang, Y. Liu, *et al.*, "Sending-or-not-sending with independent lasers: secure twin-field quantum key distribution over 509 km," Phys. Rev. Lett. **124**, 070501 (2020).
3. R. W. Boyd, "Chapter 4—the intensity-dependent refractive index," in *Nonlinear Optics*, R. W. Boyd, ed. (Academic Press, 1992), pp. 159–190.
4. J. Yu, X. Kuang, J. Li, *et al.*, "Giant nonlinear optical activity in two-dimensional palladium diselenide," Nat. Commun. **12**, 1083 (2021).
5. L. Clinton, T. Cubitt, B. Flynn, *et al.*, "Towards near-term quantum simulation of materials," Nat. Commun. **15**, 211 (2024).
6. S. Rautian and I. Sobel'man, "Line shape and dispersion in the vicinity of an absorption band, as affected by induced transitions," Sov. Phys. JETP **14**, 328–333 (1962).
7. B. R. Mollow, "Power spectrum of light scattered by two-level systems," Phys. Rev. **188**, 1969–1975 (1969).
8. R. E. Slusher, L. W. Hollberg, B. Yurke, *et al.*, "Observation of squeezed states generated by four-wave mixing in an optical cavity," Phys. Rev. Lett. **55**, 2409–2412 (1985).
9. M. D. Reid and D. F. Walls, "Quantum theory of nondegenerate four-wave mixing," Phys. Rev. A **34**, 4929–4955 (1986).
10. J.-S. Shiu, Z.-Y. Liu, C.-Y. Cheng, *et al.*, "Observation of highly correlated ultrabright biphotons through increased atomic ensemble density in spontaneous four-wave mixing," Phys. Rev. Res. **6**, L032001 (2024).
11. J.-K. Lin, T.-H. Chien, C.-T. Wu, *et al.*, "Observation of subnatural-linewidth biphotons in a two-level atomic ensemble," Phys. Rev. Lett. **134**, 043602 (2025).
12. K. Li, Y. Cai, J. Yan, *et al.*, "Direct manipulation of biphoton generation from the non-hermitian nature of light-matter interaction," Laser Photonics Rev. **19**, 2402149 (2025).
13. K. Li, J. Wen, Y. Cai, *et al.*, "Direct generation of time-energy-entangled w triphotons in atomic vapor," Sci. Adv. **10**, eado3199 (2024).
14. T. Chanelière, D. Wilkowski, Y. Bidel, *et al.*, "Saturation-induced coherence loss in coherent backscattering of light," Phys. Rev. E **70**, 036602 (2004).
15. S. Balik, P. Kulatunga, C. Sukenik, *et al.*, "Strong-field coherent backscattering of light in ultracold atomic 85rb," J. Mod. Opt. **52**, 2269–2278 (2005).
16. T. Wellens, B. Grémaud, D. Delande, *et al.*, "Coherent backscattering of light with nonlinear atomic scatterers," Phys. Rev. A **73**, 013802 (2006).
17. B. Grémaud, T. Wellens, D. Delande, *et al.*, "Coherent backscattering in nonlinear atomic media: quantum Langevin approach," Phys. Rev. A **74**, 033808 (2006).
18. D. V. Kupriyanov, I. M. Sokolov, and M. D. Havey, "Mesoscopic coherence in light scattering from cold, optically dense and disordered atomic systems," Phys. Rep. **671**, 1–60 (2017).
19. T. Binninger, V. N. Shatokhin, A. Buchleitner, *et al.*, "Nonlinear quantum transport of light in a cold atomic cloud," Phys. Rev. A **100**, 033816 (2019).
20. R. W. Boyd, M. G. Raymer, P. Narum, *et al.*, "Four-wave parametric interactions in a strongly driven two-level system," Phys. Rev. A **24**, 411–423 (1981).
21. P. P. Sorokin and J. H. Glownia, "Lasers without inversion (lwi) in space: a possible explanation for intense, narrow-band, emissions that dominate the visible and/or far-uv (fuv) spectra of certain astronomical objects," Astron. Astrophys. **384**, 350–363 (2002).
22. L. S. Froufe-Pérez, W. Guerin, R. Carminati, *et al.*, "Threshold of a random laser with cold atoms," Phys. Rev. Lett. **102**, 173903 (2009).
23. L. Landau and E. Lifshitz, *Statistical Physics* (Butterworth-Heinemann, 2013), Vol. **5**.
24. C. Cohen-Tannoudji, J. Dupont-Roc, and G. Grynberg, *Atom-Photon Interactions* (Wiley & Sons, Inc., 1993).
25. I. M. Sokolov, M. D. Kupriyanova, D. V. Kupriyanov, *et al.*, "Light scattering from a dense and ultracold atomic gas," Phys. Rev. A **79**, 053405 (2009).